

平成 25 年 9 月発行 American Journal of Ophthalmology

第 156 卷 第 3 号 511 頁~523 頁掲載

## **Macular Imaging in Highly Myopic Eyes with and without Glaucoma**

NORIKO NAKANO,<sup>1</sup> MASANORI HANGAI,<sup>1</sup>HISASHI NOMA,<sup>2</sup>MASAYUKI NUKADA,<sup>1</sup>  
SATOSHI MORI,<sup>1</sup>SATOSHI MOROOKA,<sup>1</sup> KOHEI TAKAYAMA,<sup>1</sup> YUGO KIMURA,<sup>1</sup>  
HANAKO OHASHI IKEDA,<sup>1</sup> TADAMICHI AKAGI,<sup>1</sup> NAGAHISA YOSHIMURA<sup>1</sup>

<sup>1</sup>Department of Ophthalmology and Visual Sciences, Kyoto University Graduate School of Medicine, 54 Kawahara-cho, Shogoin, Sakyo-ku, Kyoto 606-8507, Japan

<sup>2</sup>The Institute of Statistical Mathematics, 10-3 Midori-cho, Tachikawa, Tokyo 190-8562, Japan

Short Title: Imaging Highly Myopic Glaucomatous Eyes

Correspondence to: Masanori Hangai, MD  
Department of Ophthalmology and Visual Sciences  
Kyoto University Graduate School of Medicine  
54 Kawahara-cho  
Shogoin, Sakyo-ku  
Kyoto 606-8507, Japan  
E-mail: hangai@kuhp.kyoto-u.ac.jp

## ABSTRACT

**Purpose:** To determine how evaluations of macular structures on spectral-domain optical coherence tomography (SD-OCT) compare to those of optic disc and circumpapillary retinal nerve fiber layer (RNFL) in discriminating between highly myopic eyes with and without glaucoma.

**Design:** Retrospective comparative study.

**Methods:** The appearances of ganglion cell layer and RNFL on Spectralis macular scans and optic disc on photographs were evaluated by 2 observers. The receiver operating characteristic regression was conducted for macular ganglion cell complex and circumpapillary RNFL measurements on RTVue-100.

**Results:** Ninety highly myopic (-6.0– -15.0 diopters; mean deviation [MD],  $-5.6\pm 5.1$  dB) and 91 non-highly myopic (+1.0– -5.5 diopters; MD,  $-4.9\pm 5.7$  dB) eyes were enrolled. In highly myopic eyes (<-6 diopters), Cohen's  $\kappa$  for qualitative decisions by observers was 0.363 for photos and 0.946 for Spectralis macular scans and observers' evaluations of Spectralis macular scans were more accurate (94.5%, 94.5%,  $P<0.0001$ ) than photos (71.4%, 80.2%, respectively). In the receiver operating characteristic regression analyses assessing the influences of age, sex, MD and axial length, the better MD ( $P=0.002$ – $0.016$ ) and longer axial length ( $P=0.031$ – $0.041$ ) were significantly associated with diagnostic performances for all or some SD-OCT parameters. The receiver operating characteristic curves of average macular ganglion cell complex and circumpapillary RNFL thicknesses were comparable at low MD.

**Conclusions:** In high myopes, observers' assessments of the SD-OCT macular scans may agree better and be more accurate than observers' optic disc assessments. Glaucoma diagnostic performance of macular ganglion cell complex may be less affected by axial length compared with that of circumpapillary RNFL.

## INTRODUCTION

Myopia affects approximately 1.6 billion people worldwide, and the prevalence is expected to increase, particularly in East Asia,<sup>1-4</sup> to 2.5 billion by the year 2020.<sup>1,2</sup> Previous epidemiological studies identified myopia,<sup>5,6</sup> especially high myopia,<sup>7</sup> as a risk factor for developing glaucoma, and the risk of glaucoma increases with increasing degree of myopia.<sup>8</sup> Glaucomatous visual field (VF) defects in patients with high myopia may be worse,<sup>9</sup> more likely to threaten fixation,<sup>10,11</sup> and more likely to progress.<sup>12</sup> Thus, myopic patients are thought to be at greater risk of decreased quality of vision over their lifetime, making early glaucoma screening crucial for these patients. However, it is often difficult to evaluate the myopic optic disc, which often shows deformed shapes, such as tilting, cyclotorsion, pale appearance, shallow and/or large cups, and large areas of peripapillary atrophy (PPA).<sup>13-16</sup> Heidelberg Retinal Tomography (HRT) measurements of the optic disc

shape are poor discriminators of glaucoma in myopic eyes.<sup>17-20</sup>

Glaucomatous optic neuropathy results from damage to retinal ganglion cell axons within the optic nerve head. This leads to thinning of the retinal nerve fiber layer (RNFL), the ganglion cell layer, and the optic disc neuroretinal rim. Measurements of circumpapillary RNFL thickness can be made with optical coherence tomography (OCT) and prior studies have shown that decreased average circumpapillary RNFL thickness is a strong indicator of glaucoma.<sup>21-27</sup> Unfortunately, circumpapillary RNFL thickness is not as useful in highly myopic eyes.<sup>18,28-30</sup> This has been attributed to abnormal profiles of the circumpapillary RNFL in highly myopic eyes, including thinning<sup>28,31-33</sup> and differences in peripapillary thickness distribution<sup>34-36</sup> compared to non-highly myopic eyes. Circumpapillary RNFL profile abnormalities become more prominent with the degree of myopia,<sup>28,32,33,36</sup> axial length,<sup>28,29,33,36</sup> and optic disc tilting.<sup>34,35</sup>

Macular thickness measurements may well reflect retinal ganglion cell loss<sup>21-27,37</sup> because more than 50% of retinal ganglion cell somas are located within the macula.<sup>38</sup> Spectral-domain OCT (SD-OCT) allows reproducible thickness measurements of the 3 inner retinal layers, which include retinal ganglion cell somas and axons, also known as the ganglion cell complex (GCC).<sup>39-44</sup> Macular ganglion cell complex parameters were shown to have equal diagnostic value as circumpapillary RNFL thickness measurements in the detection of glaucoma in eyes without high myopia.<sup>39-44</sup> Importantly, the macular ganglion cell layer and RNFL have symmetrical shapes on cross-sectional images in non-glaucomatous eyes without high myopia,<sup>45,46</sup> so loss of symmetry on SD-OCT images can indicate unilateral damage to the macular ganglion cell layer and the RNFL.<sup>37,45</sup> Also, because the macula lies along the globe's optical axis, it may be that the macula is less affected by myopic globe elongation than the optic disc and peripapillary structures.

The current study examines the usefulness of macular retinal ganglion cell layer evaluations in glaucoma screening in highly myopic eyes. We first present SD-OCT images illustrating macular symmetry in highly myopic eyes without glaucoma, even in the presence of optic disc and peripapillary deformations. We also present images that illustrate macular symmetry loss in highly myopic eyes with glaucoma. Inter-observer agreement was assessed, as was the accuracy of SD-OCT image evaluation on macular appearance. The agreement and accuracy were also compared to photographic optic disc evaluations used to distinguish between glaucomatous and non-glaucomatous eyes. Finally, we evaluated the influence of demographic and anatomic factors, including axial length, on the ability to detect glaucoma based on OCT measurements of the circumpapillary RNFL and the macular ganglion cell complex.

## METHODS

This was a retrospective cross-sectional, case-control study. The study and data

accumulation were carried out with approval from the Institutional Review Board (IRB) and the Ethics Committee of Kyoto University Graduate School of Medicine and study conduct adhered to the tenets of the Declaration of Helsinki. Informed consent was obtained from subjects after the nature and possible consequences of study participation were explained.

Patients with a glaucoma diagnosis who visited the glaucoma service at Kyoto University Hospital between September 2009 and June 2010 were candidates for this study. All patients in the database had already undergone a comprehensive ophthalmic examination, including measurement of best-corrected visual acuity (BCVA, 5 m Landolt chart), refraction, keratometry, slit-lamp examination, axial length measurement (IOL Master 500, Carl Zeiss Meditec, Dublin, CA), Goldmann applanation tonometry, gonioscopy, indirect ophthalmoscopy, dilated slit-lamp optic nerve head examination, fundus photography, stereo disc photography (3-Dx simultaneous stereo disc camera, Nidek, Gamagori, Japan), red-free fundus photography (Heidelberg Retina Angiography 2 [HRA2], Heidelberg Engineering, Heidelberg, Germany), and standard automated perimetry (SAP, Humphrey Visual Field Analyzer, Carl Zeiss Meditec) with the 24-2 Swedish Interactive Threshold Algorithm (SITA) standard program.

Inclusion criteria included BCVA of at least 20/20, normal open angle on gonioscopy, reliable VF results, and good-quality SD-OCT images (clearly delineated macula and circumpapillary RNFL with acceptable signal strength). Patients with diabetes or vision threatening neurologic disease (e.g., pituitary tumor) and eyes with opaque media, intraocular disease (e.g., retinal vein occlusion, macular degeneration, epiretinal membrane, retinitis pigmentosa), prior surgery, or pathologic myopia (e.g., patchy chorioretinal atrophy, lacquer crack lesions, intrachoroidal cavitation, abrupt scleral curvature change temporal to the optic disc, choroidal neovascularization) were excluded from analyses. When both eyes of a patient were eligible, one eye was randomly chosen for the study.

Eyes were classified, according to the spherical equivalent of the refractive error, as either highly myopic (< -6.0 diopters) or non-highly myopic. Eyes in each group were further divided into glaucomatous and non-glaucomatous subgroups. Eyes were assigned to the glaucoma group if the optic disc appeared glaucomatous on stereo disc photographs or if at least 1 localized RNFL defect was evident on red-free fundus photographs. These findings must correspond to glaucomatous visual field defects, noted on SAP reports. Glaucomatous eyes were further classified as having early ( $\leq$ -6 dB) or severe ( $>$ -6 dB) Glaucoma, based on VF findings.

Eyes were assigned to the non-glaucomatous group only if they lacked any glaucomatous appearance of the optic disc, any visible RNFL defect on red-free RNFL photographs, or any visual field defect on two reliable SAP examinations. Eyes also had to have an IOP  $\leq$ 21 mmHg with no history of increased IOP and no family history of glaucoma in a first-degree relative. Some eyes showed an enlarged blind spot associated with large

peripapillary atrophy. These eyes were classified as the non-glaucomatous group.

Eligibility was determined by 3 glaucoma specialists (MH, HOI, TA) who evaluated optic disc appearance on stereo disc photographs and RNFL defects on red-free fundus photographs. Evaluators were masked to all other patient and ocular data and an eye was excluded from analyses if a consensus could not be reached. A glaucomatous appearance of the optic disc was defined as the clear presence of notching or neuroretinal rim thinning in the inferotemporal region and/or the superotemporal region such that the inferior-superior-nasal-temporal rule was not fulfilled.<sup>7</sup> A localized RNFL defect was classified as glaucomatous when its width at a 1-disc-diameter distance from the edge of the disc was larger than a major retinal vessel, it diverged from the edge of the optic disc in an arcuate or wedge shape, and it could not be explained by any cause other than glaucoma.

### **Visual Field Testing**

Visual field results were considered reliable if they had a fixation loss  $\leq 15\%$ , a false positive rate  $\leq 15\%$ , and a false negative rate  $\leq 15\%$ . Anderson-Patella's criteria were used to define abnormal VF results on SAP and included the following: glaucoma hemifield test (GHT) outside normal limits, pattern standard deviation (PSD) probability  $< 5\%$ , or a cluster of 3 or more adjacent non-edge points in typical glaucomatous locations that did not cross the horizontal meridian, all of which were depressed on the pattern deviation plot at a  $P < 5\%$ , one of which was depressed at a  $P < 1\%$  level confirmed on 2 reliable consecutive tests. We excluded eyes with VF defects that did not correspond to typical glaucomatous optic disc appearance and any atypical non-glaucomatous visual field defects, such as a superotemporal peripheral defect or a generalized reduction.<sup>54</sup>

### **Macular Assessment by Spectral-Domain Optical Coherence Tomography**

The Spectralis™ HRA+OCT system (Heidelberg Engineering, Heidelberg, Germany) produces clear retinal layer images in which ganglion cell layer and RNFL boundaries are clearly distinguishable (Figure 1).<sup>45</sup> These were used to evaluate the appearance of single retinal layers (e.g., ganglion cell layer, RNFL) in the macula. This instrument employs confocal laser scanning ophthalmoscopy, which enables real-time 3D tracking of eye movements. The eye tracking system allows accurate averaging of up to 100 B-scans (7  $\mu\text{m}$  axial resolution) acquired at an identical location of interest on the retina, which efficiently reduces speckle noise.<sup>45</sup> However, the software for this instrument does not automatically examine the macular ganglion cell complex. To measure the circumpapillary RNFL and macular ganglion cell complex thickness, the RTVue-100 system (software version 4.0.0.143, Optovue, Fremont, CA) was used, which allows reproducible automated measurement of these structures.<sup>39,40,42</sup>

### **Spectralis Imaging of Macular Layer Structures**

Each B-scan consists of 1,536 A-scans, providing a digital transverse sampling resolution of 5  $\mu\text{m}$  per pixel. For macular imaging, we performed 19 vertical scans (approximately 9 mm in length) at intervals of 240  $\mu\text{m}$  (Figure 1). For circumpapillary RNFL imaging, we performed a circle scan, consisting of 1,536 A-scans, with a diameter of 3.46 mm centered on the optic disc. Fifty scans were acquired along each scan line and averaged.

### **Interobserver Agreement and Accuracy of Optic Disc and Macular Evaluations**

Stereo disc photographs/color fundus photographs and Spectralis OCT macular images were separately and independently evaluated by 2 glaucoma specialists (SM, MN) in a masked fashion. For photographic evaluations, 2 observers classified each eye into 1 of 3 following categories: non-glaucomatous, glaucomatous, or hard to determine. The, hard to determine classification, was used only if a glaucomatous/non-glaucomatous decision could not be made because of severe myopic optic disc deformation.

Macular appearance was evaluated on Spectralis images, as described previously.<sup>45</sup> Briefly, evaluators were asked to compare macular ganglion cell layer and RNFL appearance in the superior and inferior hemispheres for symmetry of shape (Figure 1). The evaluators classified the eyes as not glaucomatous (normal of the macular ganglion cell layer and RNFL appearance with symmetry in the 2 hemispheres), glaucomatous (asymmetrical or diminished macular ganglion cell layer and RNFL), or hard to determine.

Agreement between evaluators was considered to occur if both observers classified the eye as glaucomatous or non-glaucomatous. A disagreement occurred if the classifications did not agree or when both observers could not decide (hard to determine).

Classification results were judged to be correct when eyes with a glaucoma diagnosis were classified as glaucomatous and eyes without a glaucoma diagnosis were classified as non-glaucomatous. Classification results were deemed incorrect when the eyes with glaucoma were classified as non-glaucomatous and vice versa. Eyes that were classified as, "hard to determine," were also regarded to be incorrectly classified.

### **Spectral-Domain Optical Coherence Tomography Measurements**

The RTVue-100 SD-OCT system has a depth resolution of approximately 5  $\mu\text{m}$ . Imaging was performed by a well-trained examiner after pupillary dilatation, with the examiner rejecting any scans that had motion artifacts (discontinuous jump), poor centration, or poor focus. Images outside of the acquisition frame were also rejected and only good-quality images (signal strength index [SSI] scores  $\geq 40.0$ ) were accepted, as suggested by the manufacturer.

Circumpapillary RNFL and macular ganglion cell complex thickness were automatically calculated by the RTVue-100's built-in software. To measure circumpapillary

RNFL thickness, the "RNFL 3.45" scan mode was used. In this mode, 4 circular scans (1,024 A-scans/scan) are acquired 3.45 mm from the center of the optic disc and the results are averaged. To measure macular ganglion cell complex thickness, we used the scan mode for ganglion cell complex analysis, which acquires 14,928 A-scans over a 7-mm square area in 0.58 s with 15 vertical scans collected at 0.5-mm intervals. The center of the ganglion cell complex scan was shifted 1.0 mm temporally to improve sampling of the temporal periphery. After scanning in ganglion cell complex mode, the RTVue-100 software automatically calculates the mean thickness of the ganglion cell complex within the central 6-mm diameter area of the macula.

The "focal loss volume (FLV)" and "global loss volume (GLV)", which are new RTVue-100 software ganglion cell complex scan parameters, were also computed. The focal loss volume is the integral of deviation in areas of significant focal ganglion cell complex loss, and GLV is the sum of negative fractional deviations over the entire scan area. The quality of ganglion cell complex and circumpapillary RNFL segmentation in all B-scans was checked with the criteria of Ishikawa, et al.<sup>47</sup> Eyes with segmentation failures were excluded from analyses.

### Statistical Analyses

Data for non-glaucomatous, early glaucoma, and severe glaucoma groups were compared using analysis of variance (ANOVA) followed by Scheffé's test as a posthoc comparison. Fisher's exact test was used to evaluate for gender distribution differences between highly and non-highly myopic groups and between non-glaucomatous, early glaucomatous and severely glaucomatous groups. Cohen's Kappa ( $\kappa$ ) was computed to evaluate interobserver agreement in glaucoma/non-glaucoma classifications in eyes with and without high myopia (value <0 indicated no agreement, value of 0–0.20 indicated slight agreement, 0.21–0.40 indicated fair agreement, 0.41–0.60 indicated moderate agreement, 0.61–0.80 indicated substantial agreement, and 0.81–1.00 indicated almost perfect agreement). McNemar's test was used to evaluate the statistical significance of differences in the number of eyes correctly classified, based on photographs or OCT images. The above statistical analyses were performed using PASW Statics software (version 17.0, SPSS, Inc., Chicago, IL).

A receiver operating characteristic regression analysis was done according to the methods of Alonzo and Pepe,<sup>48</sup> and Janes, et al.<sup>49</sup> We considered the following receiver operating characteristic regression model:

$$\text{Receiver operating characteristic } (t) = \Phi [\alpha_0 + \alpha_1 \Phi^{-1}(t) + \alpha_2 \text{Age} + \alpha_3 \text{Sex} + \alpha_4 \text{MD} + \alpha_5 \text{AL} + \alpha_6 \text{SSI}]$$

where,  $\Phi$  = probit function, MD = visual field mean deviation, AL = axial length, and SSI = signal strength index. We conducted the analyses using R version 2.15.2. The level of

significance for all tests was set at  $P < 0.05$ .

## RESULTS

During the enrollment period, 418 eyes of 248 patients (220 eyes of 127 patients without high myopia, 198 eyes of 121 patients with high myopia) met the study inclusion criteria. After matching VF defects (none, early, advanced) to clinical appearance in eyes with and without high myopia, a final study group of 90 eyes from 90 patients (37 men, 53 women) with high myopia (spherical equivalent: -6.0 to -15.0 diopters) and 91 eyes from 91 patients (42 men, 49 women) without high myopia (spherical equivalent: +1.0 to -5.5 diopters, Table 1) was obtained. In the early glaucoma groups, single hemifield VF defects were observed in 20 of 31 (64.5%) non-highly myopic eyes and 25 of 30 (16.7%) highly myopic eyes. In the severe glaucoma groups, 9 of 30 (30.0%) non-highly myopic eyes and 17 of 32 (53.1%) highly myopic eyes had single hemifield VF defects. The number of eyes with small and large optic discs is summarized in Supplementary Table 1.

### Optic Disc and Macular Appearance in Highly Myopic Eyes

The photographic appearance of the optic disc, including disc size, tilting, cyclotorsion, and shape, was highly variable in highly myopic eyes, regardless of VF defect severity (Figures 2–4). The area of peripapillary atrophy also varied in size and circumferential extent (Figures 2–4).

On Spectralis OCT images, the appearance of the ganglion cell layer and the RNFL in the macula was vertically symmetrical in both the superior and inferior hemispheres among non-glaucomatous eyes, regardless of optic disc size or deformation (Figure 2, Supplementary Figure 1). In highly myopic eyes with glaucoma, the ganglion cell layer and the RNFL in the macula had greater thinning in regions corresponding to VF losses (Figures 1, 3, 4). In many eyes with early VF defects, apparent damage/thinning was seen in the macular ganglion cell layer and the RNFL in either the inferior or superior hemisphere (Figure 3).

### Anomalous Circumpapillary Retinal Nerve Fiber Layer Images in Highly Myopic Eyes

The circumpapillary RNFL in eyes with high myopia varied in height. The circumpapillary RNFL was most commonly highest in the nasal quadrant and lowest in the temporal quadrant, thus presenting with a dome-like appearance (Figure 5). The most temporal portion of a severely elongated circumpapillary RNFL was seen in the inferior half of the image acquisition frame and generally had low signal intensity.

## Subjective Assessments

### *Inter-observer Agreement*

Cohen's  $\kappa$  in all eyes without high myopia was 0.926 for disc photographic classification and 0.951 for Spectralis OCT image classification. Cohen's  $\kappa$  in all eyes with high myopia was 0.363 for disc photos and 0.946 for Spectralis OCT images. Among eyes with high myopia, the rate of agreement was significantly higher for classifying Spectralis images (97.8%) compared to disc stereo photographs (64.4%,  $P < 0.0001$ ).

As shown in Table 2, agreement was excellent when classifying eyes without high myopia (93.3–100%), poor for photographic classification of eyes with high myopia (56.7–78.1%), and excellent for Spectralis OCT macular image classification (96.4–100%) of eyes with high myopia. Interobserver agreement was significantly better for classification with Spectralis OCT images than with disc photographs in eyes with high myopia with normal VFs or early VF defects (Table 2).

### *Accuracy of Evaluation*

In eyes without high myopia, glaucomatous or non-glaucomatous classifications based on disc photographs (100% and 96.7%, respectively) and Spectralis macular images (98.9% and 98.9%, respectively) was almost perfect for the 2 observers. In each VF results subgroup, the classification was also almost perfect in eyes without high myopia (Table 2).

In all highly myopic eyes, photograph classification was less accurate in both the glaucoma and non-glaucoma (71.4% and 80.2%, respectively) groups than Spectralis OCT image classification (94.5% and 94.5%, respectively,  $P < 0.0001$  for both observers). In each VF results subgroup of highly myopic eyes, one specialist had many false-negative classifications in eyes with early VF defects, while the other had many false-positive classifications (Table 2). In contrast, both specialists had good-to-excellent accuracy for classifications of highly myopic eyes based on Spectralis OCT image evaluations (Table 2).

## **Objective Assessments**

### *Erroneous Segmentation in Circumpapillary Retinal Nerve Fiber Layer Due to Myopic Deformation*

Apparent errors in segmentation (software generation of boundary lines) for the circumpapillary RNFL were observed in 13 (7.2%) of 181 eyes, but were not seen in macular ganglion cell complex segmentation. Errors were only found in eyes with high myopia (spherical equivalent, median = -11.5 diopters [range: -6.5 to -12.75 diopters]; axial length, median = 27.5 mm [range: 26.59–29.05 mm]). Segmentation errors seemed to be caused by inclusion of areas with peripapillary atrophy on the circumpapillary circle scan in 9 eyes (Figure 5, Top and Second row) and poor signal strength from the temporal circumpapillary RNFL being located in the inferior portion of the OCT acquisition frame ( $n = 4$  eyes, Figure 5, Third row and Bottom). The segmentation line in these regions seemed to stray away from RNFL boundaries. Some lines appeared to be pulled inferiorly, due to high scleral reflectivity

within the peripapillary atrophy, while others were displaced into other parts within the retina that had low signal intensity.

### **Average Structural Measures**

Mean  $\pm$  standard deviation (SD) values were calculated after exclusion of eyes with erroneous circumpapillary RNFL segmentation (Supplementary Table 2).

### **Receiver Operating Characteristic Curve Regression Analysis**

The receiver operating characteristic regression analysis was conducted after excluding eyes with erroneous circumpapillary RNFL segmentation (Table 3). Modeling covariates (e.g., age, sex, MD, axial length, signal strength index), revealed that better MD values were significantly associated with a worse diagnostic performance, as indicated by receiver operating characteristic curves for all of SD-OCT parameters. For circumpapillary RNFL thickness, a longer axial length was significantly, or likely, associated with a worse diagnostic performance. For macular ganglion cell complex parameters, a longer axial length was significantly associated with a worse diagnostic performance, for global loss volume only.

To visualize the effects of MD and axial length on receiver operating characteristic curves, receiver operating characteristic curves on the representative MD and axial length values are shown in Supplementary Figure 2. The receiver operating characteristic curves in average circumpapillary RNFL and macular ganglion cell complex thicknesses were almost similar at a MD level of -4 dB, but those of average circumpapillary RNFL were better than those of macular ganglion cell complex at MD levels of -10 and -20 dB.

## **DISCUSSION**

When evaluating highly myopic eyes, evaluations of macular appearance on Spectralis OCT images were more reliable and accurate than those based on stereo disc photographs. The Spectralis macular images demonstrated that macular structures are symmetrical, and not distorted, in highly myopic eyes without glaucoma, regardless of highly variable optic disc distortion or peripapillary atrophy. This macular appearance in non-glaucomatous eyes<sup>38,45,46,50</sup> may have favored a better reproducibility and accuracy. Severe loss of retinal ganglion cells<sup>51,52</sup> or severe thinning of the ganglion cell layer and RNFL in localized areas within the macula occurs, even in eyes with early glaucomatous VF defects.<sup>37,45</sup> This abnormality was easily detected when compared to the symmetrical macular appearance in highly myopic non-glaucomatous eyes.

It should be noted that our glaucomatous subjects, particularly those in the early glaucomatous groups, included a high percentage of eyes with VF defects confined to a single hemifield. This may have enhanced the detection of structural asymmetry on macular

images and facilitated the reviewer's glaucomatous/non-glaucomatous classification. Nevertheless, the high percentage of eyes with VF defects confined to a single hemifield did not appear to favor optic disc assessment in highly myopic eyes.

In the current study, we also illustrated that critical segmentation errors occurred in circumpapillary RNFL measurement in highly myopic eyes only. This was not the case for macular ganglion cell complex measurements. The causes for errors were related to myopic peripapillary changes, influenced by inclusion of areas with peripapillary atrophy that crossed the circumpapillary RNFL circle scan and/or had low signal intensity in the temporal region due to severe tilting of the peripapillary sclera. The circumpapillary RNFL image was, at times, so axially elongated that the temporal region appeared in the bottom of the image acquisition frame, where SD-OCT technology is known to have poor signal strength.<sup>53</sup> Although earlier studies did not report this difficulty in highly myopic eyes,<sup>54,55</sup> this finding may be important and should not be ignored.

After excluding eyes with circumpapillary RNFL segmentation errors, a better MD value was significantly associated with a worse diagnostic performance in all circumpapillary RNFL and macular ganglion cell complex parameters. Additionally, a longer axial length was associated with a worse diagnostic performance for all circumpapillary RNFL and for global loss volume in macular ganglion cell complex parameters. These results suggest that circumpapillary RNFL parameters are less accurate, diagnostically, in eyes with earlier glaucoma and higher myopia, and that macular ganglion cell complex thickness and focal loss volume are less affected by higher myopia.

Our results disagree with those of Kim, et al.,<sup>54</sup> who found that areas under receiver operating characteristic curves for circumpapillary RNFL and macular ganglion cell complex thickness were almost equivalent in eyes with and without high myopia. However, their study did not control for age, axial length, MD or signal strength index. In particular, their highly myopic subjects averaged more than 10 years younger than their non-highly myopic subjects.<sup>54</sup> Age-related thinning of the circumpapillary RNFL<sup>56,57</sup> and macular ganglion cell complex<sup>46,58</sup> may significantly influence results in these study subjects.

Although we controlled for age in receiver operating characteristic regression analyses, the age difference between highly myopic and non-highly myopic groups may have had a significant effect on our subjective assessments. A possible interpretation of the intergroup age difference is that VF defects appear earlier in glaucomatous eyes with high myopia than in those without high myopia.<sup>9</sup> Another possible interpretation is that high myopia, itself, may contribute to VF defects in younger patients. High myopia was recently found to be a high-risk factor for progressive VF defects that could not be explained by myopic macular lesions.<sup>59</sup> In the current study, we excluded eyes with non-glaucomatous visual field defects and those with pathologic myopia lesions. However, it still may be that some eyes had non-glaucomatous damage, which was responsible for the younger mean

age of highly myopic groups.

It should be noted that our non-glaucomatous subjects were not a group of normal subjects specifically enrolled in this study. These subjects were examined in our glaucoma service and found to have no evidence of glaucoma.

It was difficult to define glaucoma in highly myopic eyes. We included optic disc appearance in enrollment criteria, but the main goal of our study was to compare the diagnostic capabilities of structural outcomes. The motivation for performing this study was derived from the fact that evaluating optic disc appearance can be difficult in highly myopic eyes. To maximize accuracy, the optic disc was classified as, "glaucomatous," only when the abnormal findings corresponded to glaucomatous VF defects. In contrast, if VF test results are used alone to define glaucoma, eyes with preperimetric glaucoma are classified into the non-glaucomatous group.

We could not consider the size and shape of the optic disc because of the limited scale of the study. For example, small and large discs are often difficult to evaluate, and we must therefore be aware of the possibility that the inclusion of such optic discs may have biased our results. However, the number of eyes with small or large discs was small and did not differ greatly among the groups.

Magnification effects from increased axial length could not be corrected by the RTVue-100 software. In general, axial length affects lateral length measurements (magnification effect) with OCT, which consequently affects the size of the measurement circle on circumpapillary RNFL scans and macular ganglion cell complex area. We must consider these magnification effects, particularly when comparing eyes with and without high myopia.

In conclusion, subjective assessment of SD-OCT macular serial scans may be useful for supporting a glaucoma diagnosis made through photographic disc assessment and software analysis in highly myopic eyes. The diagnostic performance of macular ganglion cell complex thickness and focal loss volume in detecting glaucoma may be less affected by axial length than circumpapillary RNFL thickness measurements, but these macular parameters were comparable to circumpapillary RNFL parameters at early MD levels. These findings must be considered when SD-OCT parameters are used for glaucoma diagnosis in highly myopic eyes.

## **ACKNOWLEDGMENTS/DISCLOSURE**

*a. Funding/Support:* This research was supported, in part, by a Grant-in-Aid for Scientific Research (20592038) from the Japan Society for the Promotion of Science (JSPS), Tokyo, Japan.

*b. Financial Disclosure:* Masanori Hangai is a paid advisory board member for NIDEK and received consulting fees from Topcon, lecture fees from Heidelberg Engineering and Santen, and research funding from Nidek, Topcon, and Canon. Nagahisa Yoshimura is a paid advisory board member for NIDEK and has received lecture fees and research funding from Nidek, Topcon, and Canon. None of the other authors have any financial disclosure.

*c. Contributions by Authors in each of these areas:* Design of the study by NN and MH; data collection by SM, KT, YK; analysis and interpretation by NN, MH, HN, MN, SM, HOI, TA; writing of the article by NN and MH; critical revision of the article by NH, NY; and final approval of the article by NN, MH, HN, MN, SM, SM, KT, YK, HOI, TA, and NY.

*d. Other Acknowledgments:* None.

## REFERENCES

1. Lin LK, Shih YF, Tsai CR, et al. Epidemiologic study of ocular refraction among school children in Taiwan in 1995. *Optom Vis Sci* 1999;76(5):275-81.
2. Ling SL, Chen AJ, Rajan U, et al. Myopia in ten year old children: a case control study. *Singapore Med J* 1987;28(4):288-92.
3. Au Eong KG, Tay TH, Lim MK. Race, culture and myopia in 110,236 young Singaporean males. *Singapore Med J* 1993;34(1):29-32.
4. He M, Xu J, Yin Q, et al. Need and challenges of refractive correction in urban Chinese school children. *Optom Vis Sci* 2005;82(4):229-34.
5. Mitchell P, Hourihan F, Sandbach J, Wang JJ. The relationship between glaucoma and myopia: the Blue Mountains Eye Study. *Ophthalmology* 1999;106(19):2010-5.
6. Suzuki Y, Iwase A, Araie M, et al. Risk factors for open-angle glaucoma in a Japanese population: The Tajimi study. *Ophthalmology* 2006;113(9):1613-7.
7. Xu L, Wang Y, Wang S, Wang Y, Jonas JB. High myopia and glaucoma susceptibility: The Beijing Eye Study. *Ophthalmology* 2007;114(2):216-20.
8. Marcus MW, de Vries MM, Montolio FG, Jansonius NM. Myopia as a risk factor for open-angle glaucoma: a systematic review and meta-analysis. *Ophthalmology* 2012;118(10):1989-94.
9. Perkins ES, Phelps CD. Open angle glaucoma, ocular hypertension, low-tension glaucoma, and refraction. *Arch Ophthalmol* 1982;100(9):1464-7.
10. Mayama C, Suzuki Y, Araie M, et al. Myopia and advanced-stage open-angle glaucoma. *Ophthalmology* 2002;109(11):2072-7.
11. Araie M, Arai M, Koseki N, et al. Influence of myopic refraction on visual field defects in normal tension and primary open angle glaucoma. *Jpn J Ophthalmol* 1995;39(1):60-4.
12. Chihara E, Liu X, Dong J, et al. Severe myopia as a risk factor for progressive visual field loss in primary open-angle glaucoma. *Ophthalmologica* 1997;211(2):66-71.
13. Jonas JB, Gusek GC, Naumann GO. Optic disk morphometry in high myopia. *Graefes Arch Clin Exp Ophthalmol* 1988;226(6):587-90.
14. Nicolela MT, Drance SM. Various glaucomatous optic nerve appearances: clinical correlations. *Ophthalmology* 1996;103(4):640-9.
15. Jonas JB, Dichtl A. Optic disc morphology in myopic primary open-angle glaucoma. *Graefes Arch Clin Exp Ophthalmol* 1997;235(10):627-33.
16. Tay E, Seah SK, Chan SP, et al. Optic disk ovality as an index of tilt and its relationship to myopia and perimetry. *Am J Ophthalmol* 2005;139(2):247-52.
17. Yamazaki Y, Yoshikawa K, Kunimatsu S, et al. Influence of myopic disc shape on the diagnostic precision of the Heidelberg retina tomograph. *Jpn J Ophthalmol* 1999;43(5):392-7.

18. Melo GB, Libera RD, Barbosa AS, Pereria LM, Doi LM, Melo LA Jr. Comparison of optic disk and retinal nerve fiber layer thickness in nonglaucomatous and glaucomatous patients with high myopia. *Am J Ophthalmol* 2006;142(5):858-60.
19. Abe H, Shirakashi M, Tsutsumi T, et al. Laser scanning tomography of optic discs of the normal Japanese population in a population based setting. *Ophthalmology* 2009;116(2):223-30.
20. Tong L, Chan YH, Gazzard G, et al. Heidelberg retinal tomography of optic disc and nerve fiber layer in Singapore children: variations with disc tilt and refractive error. *Invest Ophthalmol Vis Sci* 2007;48(11):4939-44.
21. Guedes V, Schuman JS, Hertzmark E, et al. Optical coherence tomography measurement of macular and nerve fiber layer thickness in normal and glaucomatous human eyes. *Ophthalmology* 2003;110(1):177-89.
22. Lederer DE, Schuman JS, Hertzmark E, et al. Analysis of macular volume in normal and glaucomatous eyes using optical coherence tomography. *Am J Ophthalmol* 2003;135(6):838-43.
23. Greenfield DS, Bagga H, Knighton RW. Macular thickness changes in glaucomatous optic neuropathy detected using optical coherence tomography. *Arch Ophthalmol* 2003;121(1):41-6.
24. Wollstein G, Schuman JS, Price LL, et al. Optical coherence tomography (OCT) macular and peripapillary retinal nerve fiber layer measurements and automated visual fields. *Am J Ophthalmol* 2004;138(2):218-25.
25. Wollstein G, Ishikawa H, Wang J, et al. Comparison of three optical coherence tomography scanning areas for detection of glaucomatous damage. *Am J Ophthalmol* 2005;139(1):39-43.
26. Medeiros FA, Zangwill LM, Bowd C, et al. Evaluation of retinal nerve fiber layer, optic nerve head, and macular thickness measurements for glaucoma detection using optical coherence tomography. *Am J Ophthalmol* 2005;139(1):44-55.
27. Ojima T, Tanabe T, Hangai M, et al. Measurement of retinal nerve fiber layer thickness and macular volume for glaucoma detection using optical coherence tomography. *Jpn J Ophthalmol.* 2007;51(3):197-203.
28. Leung CK, Mohamed S, Leung KS, et al. Retinal nerve fiber layer measurements in myopia: An optical coherence tomography study. *Invest Ophthalmol Vis Sci* 2006;47(12):5171-6.
29. Vernon SA, Rotchford AP, Negi A, Ryatt S, Tattersal C. Peripapillary retinal nerve fibre layer thickness in highly myopic Caucasians as measured by Stratus optical coherence tomography. *Br J Ophthalmol* 2008; 92(8):1076-80.

30. Qiu KL, Zhang MZ, Leung CK, et al. Diagnostic classification of retinal nerve fiber layer measurement in myopic eyes: a comparison between time-domain and spectral-domain optical coherence tomography. *Am J Ophthalmol* 2011;152(4):646-53.
31. Kim MJ, Lee EJ, Kim TW. Peripapillary retinal nerve fibre layer thickness profile in subjects with myopia measured using the Stratus optical coherence tomography. *Br J Ophthalmol* 2010;94(1):115-20.
32. Mohammad Salih PA. Evaluation of peripapillary retinal nerve fiber layer thickness in myopic eyes by spectral-domain optical coherence tomography. *J Glaucoma* 2012;21(1):41-4.
33. Rauscher FM, Sekhon N, Feuer WJ, et al. Myopia affects retinal nerve fiber layer measurements as determined by optical coherence tomography. *J Glaucoma* 2009;18(7):501-5.
34. Hwang YH, Yoo C, Kim YY. Myopic optic disc tilt and the characteristics of peripapillary retinal nerve fiber layer thickness measured by spectral-domain optical coherence tomography. *J Glaucoma* 2012;21(4):260-5.
35. Hwang YH, Yoo C, Kim YY. Characteristics of peripapillary retinal nerve fiber layer thickness in eyes with myopic optic disc tilt and rotation. *J Glaucoma* 2012;21(6):394-400.
36. Kang SH, Hong SW, Im S, Lee S, Ahn MD. Effect of myopia on the thickness of the retinal nerve fiber layer measured by Cirrus HD optical coherence tomography. *Invest Ophthalmol Vis Sci* 2010;51(8):4075-83.
37. Wang M, Hood DC, Cho JS, et al. Measurement of local retinal ganglion cell layer thickness in patients with glaucoma using frequency-domain optical coherence tomography. *Arch Ophthalmol* 2009;127(7):875-81.
38. Curcio CA, Allen KA. Topography of ganglion cells in human retina. *J Comp Neurol* 1990;300(1):5-25.
39. Tan O, Chopra V, Lu AT, et al. Detection of macular ganglion cell loss in glaucoma by Fourier-domain optical coherence tomography. *Ophthalmology* 2009;116(12):2305-14.
40. Seong M, Sung KR, Choi EH, et al. Macular and peripapillary retinal nerve fiber layer measurements by spectral domain optical coherence tomography in normal-tension glaucoma. *Invest Ophthalmol Vis Sci* 2010;51(3):1446-52.
41. Mori S, Hangai M, Sakamoto A, Yoshimura N. Spectral-domain optical coherence tomography measurement of macular volume for diagnosing glaucoma. *J Glaucoma*. 2010;19(8):528-34.
42. Rao HL, Zangwill LM, Weinreb RN, et al. Comparison of different spectral domain optical coherence tomography scanning areas for glaucoma diagnosis. *Ophthalmology* 2010;117(9):1692-9.
43. Kotera Y, Hangai M, Hirose F, Mori S, Yoshimura N. Three-dimensional imaging of

- macular inner structures in glaucoma by using spectral-domain optical coherence tomography. *Invest Ophthalmol Vis Sci* 2011;52(3):1412-21.
44. Nakatani Y, Higashide T, Ohkubo S, et al. Evaluation of macular thickness and peripapillary retinal nerve fiber layer thickness for detection of early glaucoma using spectral domain optical coherence tomography. *J Glaucoma* 2011;20(4):252-9.
  45. Nakano N, Hangai M, Nakanishi H, et al. Macular ganglion cell layer imaging in preperimetric glaucoma with speckle noise-reduced spectral domain optical coherence tomography. *Ophthalmology* 2011;118(12):2414-26.
  46. Ooto S, Hangai M, Tomidokoro A, et al. Effects of age, sex, and axial length on the three-dimensional profile of normal macular layer structures. *Invest Ophthalmol Vis Sci* 2011;52(12):8769-79.
  47. Ishikawa H, Stein DM, Wollstein G, et al. Macular segmentation with optical coherence tomography. *Invest Ophthalmol Vis Sci* 2005;46(6):2012-17.
  48. Alonzo TA, Pepe MS. Distribution-free ROC analysis using binary regression techniques. *Biostatistics* 2002;3(3):421-432.
  49. Janes H, Longton G, Pepe MS. Accommodating covariates in receiver operating characteristic analysis. *Stata J* 2009;9(1):17-39.
  50. Bagga H, Greenfield DS, Knighton RW. Macular symmetry testing for glaucoma detection. *J Glaucoma* 2005;14(5):358-63.
  51. Quigley HA, Dunkelberger GR, Green WR. Retinal ganglion cell atrophy correlated with automated perimetry in human eyes with glaucoma. *Am J Ophthalmol* 1989;107(5):453-64.
  52. Kerrigan-Baumrind LA, Quigley HA, Pease ME, et al. Number of ganglion cells in glaucoma eyes compared with threshold visual field tests in the same persons. *Invest Ophthalmol Vis Sci* 2000;41(3):741-8.
  53. Potsaid B, Baumann B, Huang D, et al. Ultrahigh speed 1050 nm swept source/Fourier domain OCT retinal and anterior segment imaging at 100,000 to 400,000 axial scans per second. *Opt Express* 2010;18(19):20029-48.
  54. Kim NR, Lee ES, Seong GJ, et al. Comparing the ganglion cell complex and retinal nerve fibre layer measurements by Fourier domain OCT to detect glaucoma in high myopia. *Br J Ophthalmol* 2011;95(8):1115-21.
  55. Shoji T, Sato H, Ishida M et al. Assessment of glaucomatous changes in subjects with high myopia using spectral domain optical coherence tomography. *Invest Ophthalmol Vis Sci* 2011;52(2):1098-102.
  56. Hirasawa H, Tomidokoro A, Araie M, et al. Peripapillary retinal nerve fiber layer thickness determined by spectral-domain optical coherence tomography in ophthalmologically normal eyes. *Arch Ophthalmol* 2010;128(11):1420-6.
  57. Leung CK, Yu M, Weinreb RN, et al. Retinal nerve fiber layer imaging with

spectral-domain optical coherence tomography a prospective analysis of age-related loss. *Ophthalmology* 2012;119(4):731-7.

58. Kim NR, Kim JH, Lee J, et al. Determinants of perimacular inner retinal layer thickness in normal eyes measured by Fourier-domain optical coherence tomography. *Invest Ophthalmol Vis Sci* 2011;52(6):3413-8.
59. Ohno-Matsui K, Shimada N, Yasuzumi K, et al. Long-term development of significant visual field defects in highly myopic eyes. *Am J Ophthalmol* 2011;152(2):256-65.

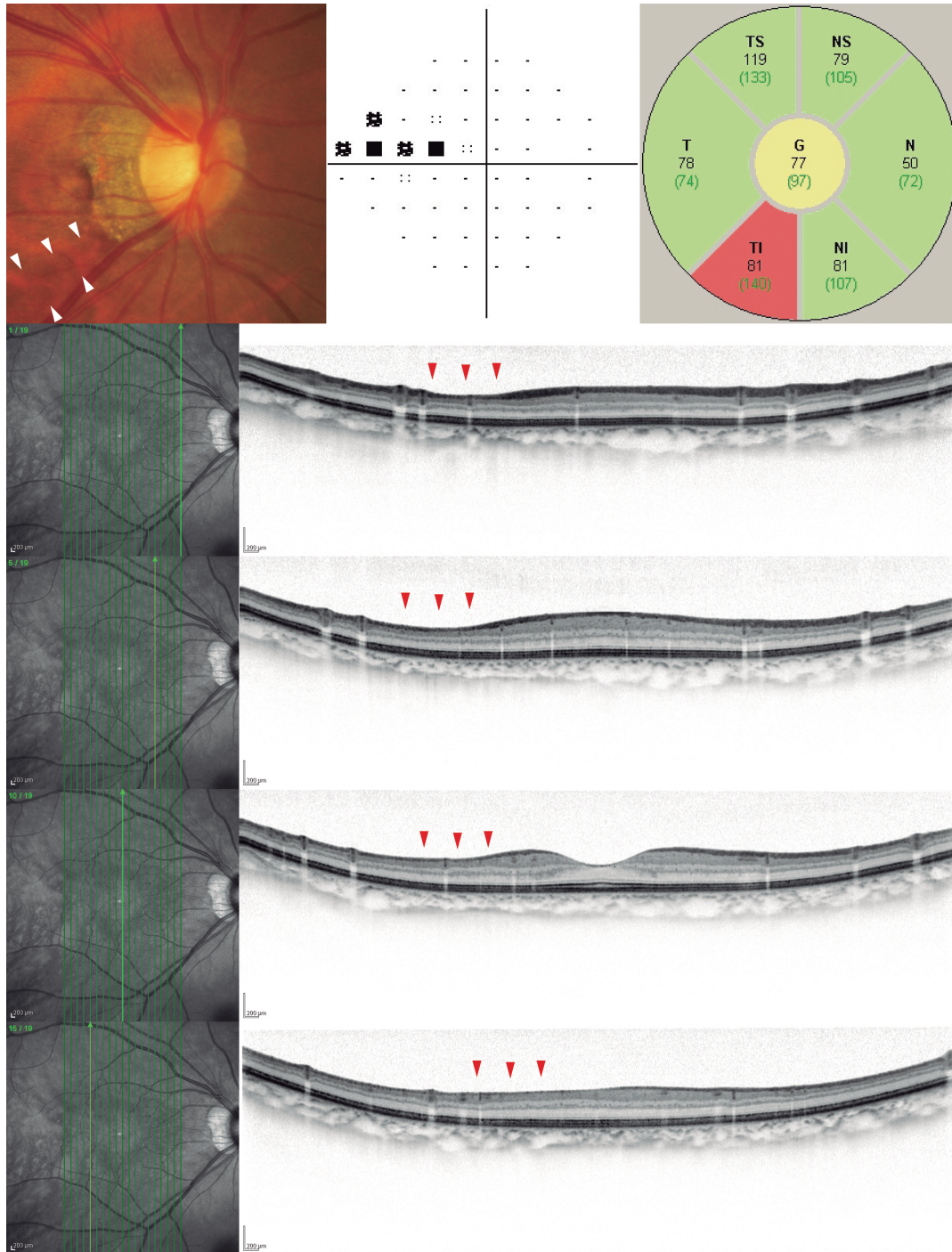


**Figure 1.** Appearance of the macula on Spectralis serial vertical scans in a highly myopic eye with glaucoma. (Top left) A color disc photograph. White arrowheads indicate retinal nerve fiber layer (RNFL) defects. (Top center) Humphrey 24-2 Swedish Interactive Threshold Algorithm standard pattern deviation map. (Top right) Spectralis circumpapillary RNFL thickness map. Red = abnormal thinning (mean thickness less than the lower 99% confidence interval [CI] value of normal eyes). Yellow = borderline thinning (mean thickness between the lower 95% and lower 99% CI values of normal eyes). Green = within normal limits (mean thickness within the 95% CI of normal eyes). (Second, Third, and Fourth rows, and Bottom) Spectralis vertical scan images over the macula in the same eye. Images of first (Second row), fifth (Third row), tenth (Fourth row), and fifteenth (Bottom) scan lines from nasal to temporal of 19 serial vertical scans from inferior to superior (indicated by green lines in infrared images [Left] at intervals of 240  $\mu\text{m}$  are shown. Speckle noise was reduced by averaging 50 B-scans to produce each image shown. Apparent thinning of the macular ganglion cell layer and retinal nerve fiber layer is seen in the inferior hemisphere (red arrowheads) compared to the opposite (superior) hemisphere, which corresponds to the RNFL defects, visual field defects and abnormal circumpapillary RNFL thickness.

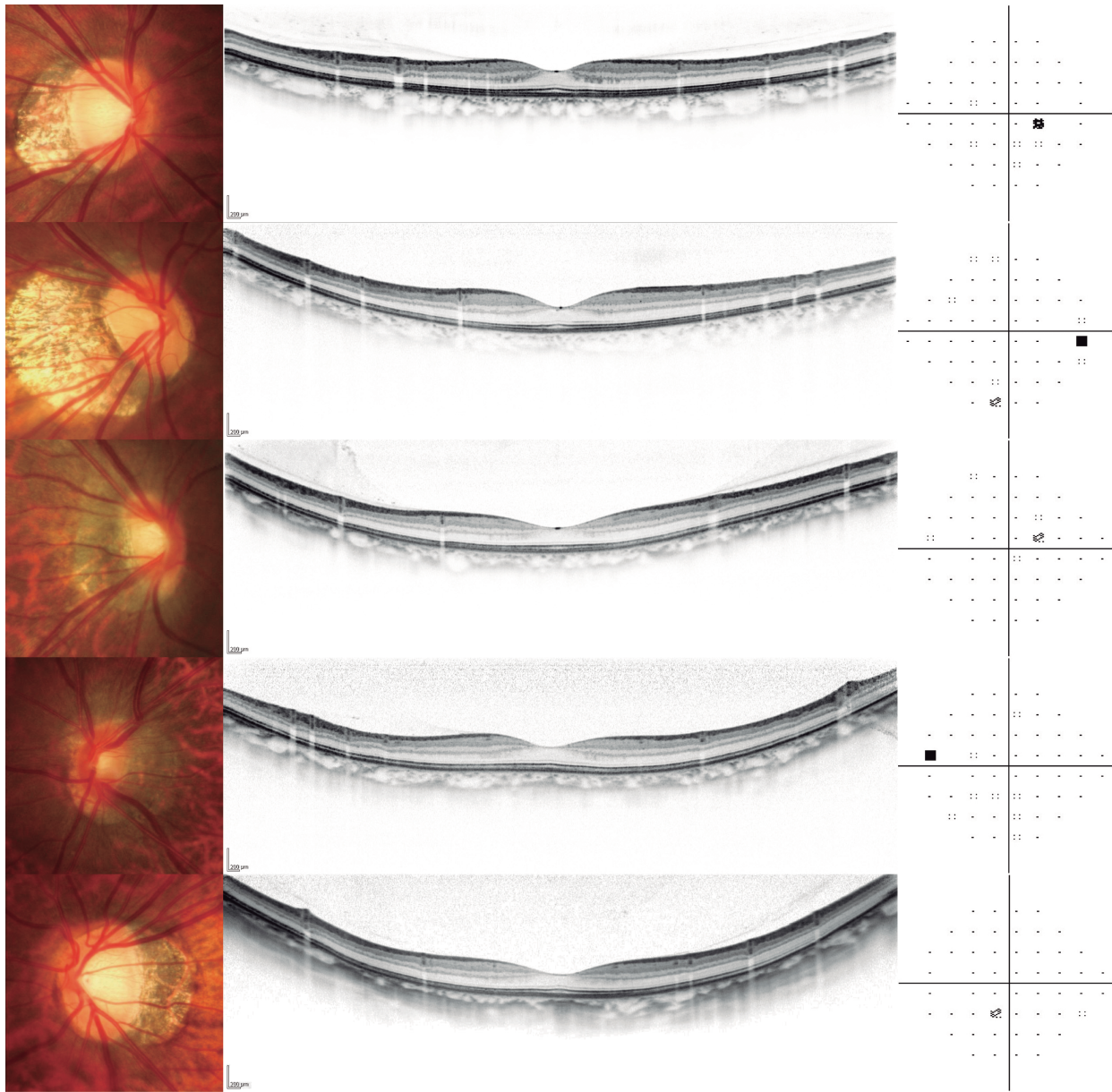


Figure2. Appearance of the macula on Spectralis scans obtained in highly myopic non-glaucomatous eyes with highly variable deformations of the optic disc and peripapillary atrophy. Color disc photographs (Left), vertical 9-mm-long Spectralis scans from inferior to superior (Center), and visual field (VF) pattern deviation maps (Right) are shown. The macula appears uniformly symmetrical across the horizontal meridian regardless of variable myopic deformations, such as disc tilt, rotation, size, and peripapillary atrophy. There is some bowing of the posterior pole, but the macular region (6 mm) is almost all within the superior half of the image acquisition frame, where good signal intensity can be obtained.

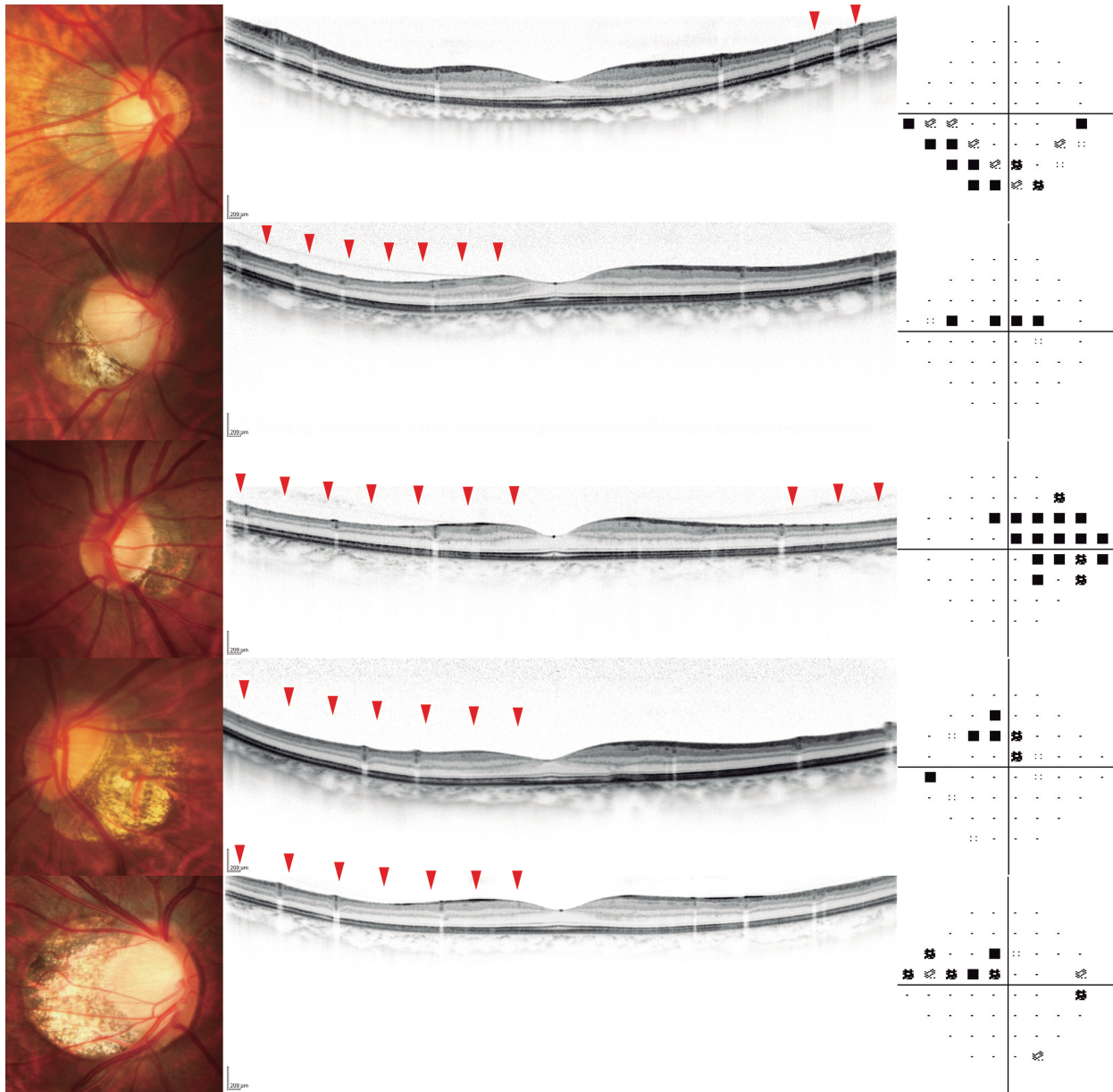


Figure 3. Appearance of the macula on Spectralis scans obtained in highly myopic glaucomatous eyes with early visual field defects with highly variable deformations of the optic disc and peripapillary atrophy. Color disc photographs (Left), vertical 9-mm-long Spectralis scans from inferior to superior (Center), and visual field (VF) pattern deviation maps (Right) are shown. The ganglion cell layer and retinal nerve fiber layer appear diminished in the hemisphere (red arrowheads) corresponding to the visual field defects.

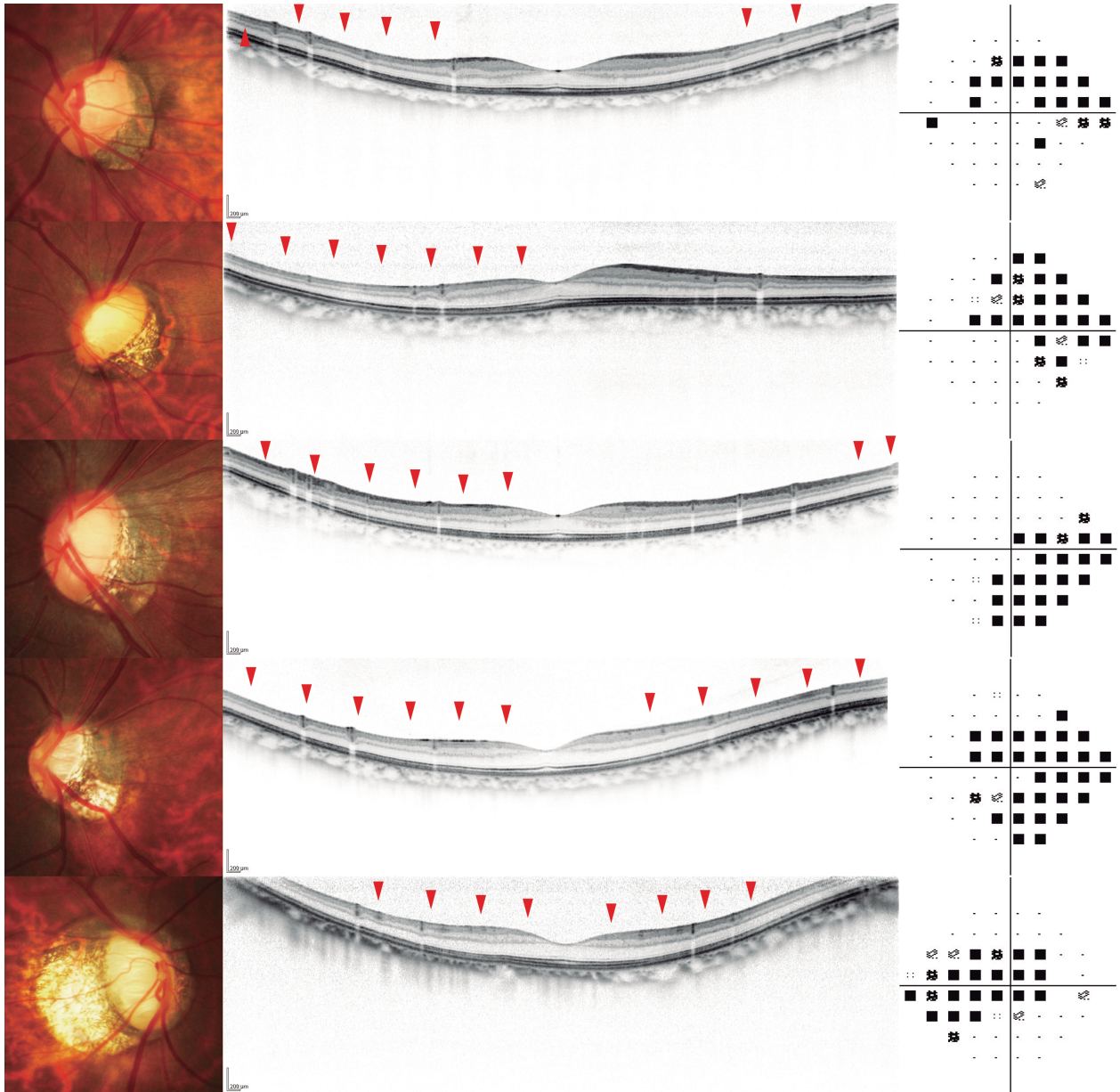


Figure 4. Appearance of the macula on Spectralis scans obtained in highly myopic glaucomatous eyes with severe visual field defects with highly variable deformations of the optic disc and peripapillary atrophy. Color disc photographs (Left), vertical 9-mm-long Spectralis scans from inferior to superior (Center), and visual field (VF) pattern deviation maps (Right) are shown. The ganglion cell layer and retinal nerve fiber layer appear diminished in the hemisphere (red arrowheads) corresponding to the visual field defects.